

# The essential mechanics of conchoidal flaking

B. COTTERELL \*, J. KAMMINGA \*\* and F.P. DICKSON \*

\* *Department of Mechanical Engineering, University of Sydney, Sydney, N.S.W. 2006, Australia*

\*\* *Department of Prehistory, Research School of Pacific Studies, Australian National University, Canberra, Australia*

(Received 24 April 1985; in revised form 15 September 1985)

## Abstract

Flaked stone tools are the most durable and therefore the most common artifacts available to archaeologists for tracing the development of early Man. However, the essential mechanics of conchoidal flake formation has not yet been described. In order to successfully create a relatively thin flake that does not terminate prematurely, the direction of the flaking force has to be reasonably precise. We show that the direction of the flaking force is determined mainly by the stiffness of the flake, the actual angle of the blow or impulse having relatively little effect. Long thin flakes can be easily produced because this direction of the flaking force is very close to that necessary to produce local symmetry at the tip of the crack propagating parallel to the surface of the stone.

## 1. Introduction

Human history before the age of metal is traced by archaeologists largely through the identification of flaked stone artifacts. In some parts of the world, such as Australia, the Stone Age lasted until well into the Nineteenth Century, and even today there are a few isolated groups of people in the world, like the Jarawa of the Andaman Islands, who still rely on stone for some of their essential tools. In fact, flaked stone artifacts are the primary evidence of cultural evolution for more than 99% of the history of the human species – they remain the single most archaeologically visible aspect of early technology and the one that most distinguishes early Man as an intelligent species.

It is a common misconception that flaked stone tools were made from rock types that could be split along well-defined cleavage planes. However, the stone types favoured for tool-making were the most homogeneous and isotropic obtainable. Early Man discovered that siliceous stone such as glassy obsidian and microcrystalline chert (one variety of which is flint) had the desirable flaking properties; the more granular materials, such as quartzite, were normally only exploited if better materials were unobtainable. In many parts of the world the best stone for tool-making was traded by sea or overland for long distances. By early Neolithic times good quality flint had become scarce in some parts of Europe and so mines ten meters deep were dug to obtain it.

In the making of stone tools primary flakes are detached from a piece of stone (called a core) either by a percussive blow with a hammer of stone or some other hard material, or by the application of a more or less impulsive pressure with a shaft of bone, antler or dense wood. Flakes thus removed often served as tools without needing further shaping. Because the path of a fracture in homogeneous and isotropic stone was predictable, a primary flake could be shaped by flaking it into a smaller tool of standard form. It is only

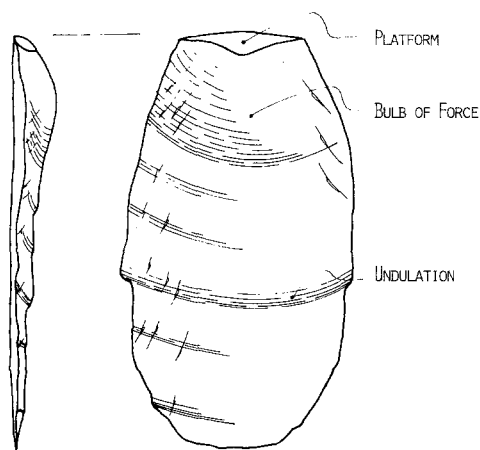


Figure 1. A conchoidal flake.

in relatively recent prehistoric times that the standardized shaping of primary flakes by retouch became in any way sophisticated.

Whatever flaking technique is used to produce a conchoidal flake the mechanics involved is virtually the same. Force applied through the convex surface of a hard object to a small area or platform near the margin of the core produces a partial Hertzian cone crack [1]. As the crack grows it curves inward to form what will appear on the upper part of the detached flake as a swelling, which is called the bulb of force. The crack quickly flattens out beyond the bulb of force and propagates almost parallel to the surface of the core. If the surface of the core under which the fracture forms is flattish, the fracture will spread sideways to produce a thin shell-like or "conchoidal" flake (see Fig. 1). Narrow blade-like flakes with very thin and sharp edges can be created by preforming a ridge down the core that will prevent the sideways spread of the fracture. What is remarkable is that such long thin flakes can be produced with relative ease. Practical experience indicates that the blow required to detach a thin flake can have a large outward component, which would be expected to make the fracture hinge outward to produce a short stubby flake of little use as a tool.

Although the fracture surface morphology of flakes is now reasonably well understood [2–5] the fundamental question of why a crack travels roughly parallel to the surface of the core has not been addressed. A fuller understanding of the mechanics of flaking can be expected to provide information about the prehistoric techniques of stone tool manufacture. The mechanics of flaking is at least as important to the nascent field of use-wear analysis in archaeology. During use stone tools can sustain damage in the form of small flake scars on their cutting edges. Archaeologists are currently studying this fracture along with other types of use-wear for the purpose of identifying the functions of prehistoric stone tools [5–7].

In this paper we outline the essential mechanics of conchoidal flake formation in relation to the question of why a fracture tends to run parallel to the surface of the core subsequent to the formation of the bulb of force. Although our description of crack propagation is couched in terms of conchoidal flakes, it applied equally well to flakes initiated by bending which frequently occur when a soft flaking tool is used. For ease of expression we will always refer to a flake that is being detached from a core as occurs in primary flake production, even though the mechanics applies to secondary flaking and to the detachment of a microflake from a stone tool during use.

**2. The stress intensity factor at the tip of a growing flake**

Although the complete description of flake formation must take its three-dimensional nature into account, the essential mechanics can be understood from a two-dimensional model. The initial curvature of the flake around the bulb of force will not have a significant effect on the flake's subsequent formation. Consequently, we have modelled a core with a partially detached flake as a two-dimensional square edged slab with crack running parallel to one side. To non-dimensionalize the problem we have made the flake of unit thickness. The Hertzian cone forms at the edge of the contact zone between the indenter and the core. Typically the diameter of the contact zone is small, being in the order of one or two millimeters. Therefore it is reasonable to place the point of force application at the corner of our rectilinear model of a flake (see Fig. 2). The flake force can be resolved into a direct component  $P$  (load case 1) and a transverse component  $Q$  (load case 2). Because of their possible application in engineering we have also considered a direct force applied to the centroid of the flake (load case 3) and a bending moment (load case 4). We assume that in all cases the flake is small compared with the size of the core or tool, so that the precise details of how the core is supported is unimportant. Experimental flakes formed on the edges of square glass plates show that the direction of crack is affected by the presence of the base of the core when the crack is closer than at least six times the flake thickness [2].

*2.1. The beam model*

Gross and Srawley [8] have shown that the stress intensity factor for a double cantilever beam (DCB) under symmetrical opening forces can be estimated from beam theory with

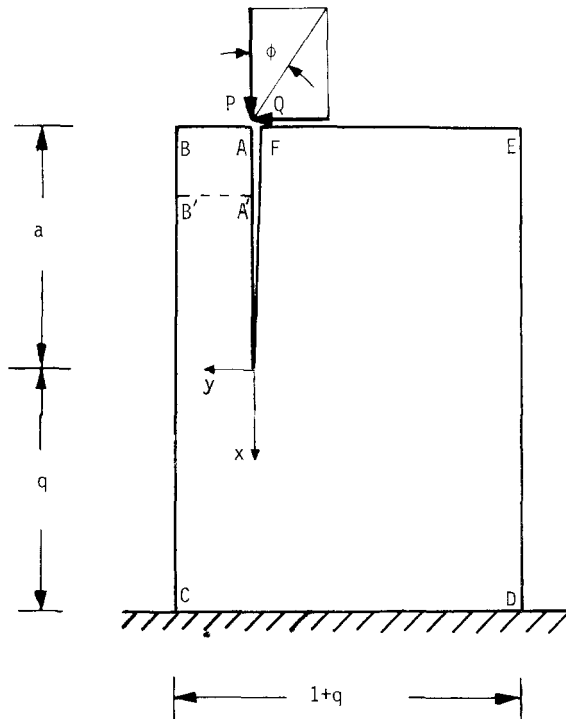


Figure 2. Two dimensional model of a conchoidal flake.

Table 1. The modulus of the stress intensity as given by simple bending theory

Load case	$\bar{K}$
	$\sqrt{2} \left\{ 1 - \frac{1}{4(q+1)} \left[ 1 + 3 \left( \frac{q-1}{q+1} \right)^2 \right] \right\}^{1/2}$
	$\sqrt{6a} \left( 1 - \frac{1}{(q-1)^3} \right)^{1/2}$
	$\frac{1}{\sqrt{2}} \left\{ 1 - \frac{1}{(q+1)} \left[ 1 + 3 \left( \frac{q}{q+1} \right)^2 \right] \right\}^{1/2}$
	$\sqrt{6} \left( 1 - \frac{1}{(q+1)^3} \right)^{1/2}$

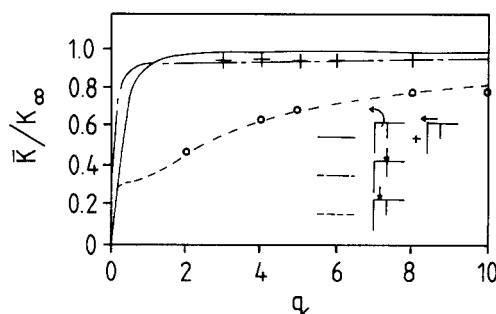


Figure 3. The modulus of the stress intensity as a function of core size.

an accuracy of better than 12% provided the length to depth ratio is greater than 5. Under antisymmetrical forces acting along the crack line the stress intensity factor obtained from beam theory is accurate to better than 1% for beams as short as twice their depth [9]. In these examples the stress intensity factor is either all mode I or mode II. There is no symmetry in flake detachment and consequently the stress intensity factor is of mixed mode. Although the modulus  $\bar{K} = (K_I^2 + K_{II}^2)^{1/2}$  of the stress intensity factor can be obtained from beam theory the individual components cannot be separated. However, the modulus of the stress intensity factor obtained from beam theory is valuable in the subsequent analysis.

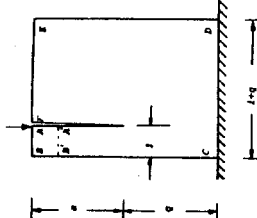
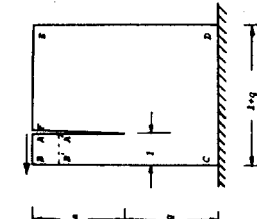
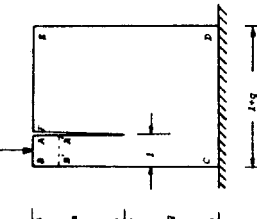
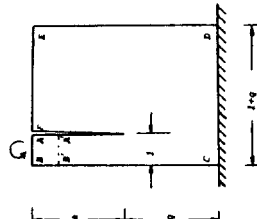
We assume that the core rests on a base where the reactions to the flaking forces are provided by direct and transverse forces acting at the centroid of the core together with a bending moment. The modulus of the stress intensity factor is obtained from the variation in bending and direct strain energy in the flake and core for an infinitesimal crack extension (see Table 1). The shear strain energy has been neglected. For large cores ( $q/a \gg 1$ ) the energy stored in the core is very small compared with that stored in the flake and the modulus of the stress intensity factor attains a limiting value  $\bar{K}_\infty$ . The effect of the core's dimensions on the stress intensity factor is shown in Fig. 3. The stress intensity factor for a flake that is loaded essentially by bending (cases 2 and 4) attains its limiting value for a quite small core, whereas the core has to be much larger for a flake under an essentially direct load (case 3). For load case 1, which is a combination of load cases 3 and 4, the stress intensity factor quickly attains more than 90% of its limiting value for a core that is no more than twice as wide as the flake, but its final limiting value is only approached extremely slowly. Even when the core is eleven times thicker than the flake, the stress intensity factor is still only 96.5% of its limiting value.

## 2.2. A boundary collocation solution for flaking

Gross and Srawley [8] have successfully used the boundary collocation technique to calculate the stress intensity factor for a double cantilever beam loaded by symmetrical opening forces. Although Gross and Srawley claimed that their empirical formula (based on the collocation solution) was accurate for beams longer than twice their depth, recent work [9] has shown that the method is accurate to within 4% for beams as short as one third their depth.

In the Gross and Srawley method of boundary collocation [8], the Williams' series expansion for the Airy stress function for the stress distribution at the tip of a crack [11] is used. The series, which in our case must include both symmetric and antisymmetric terms, exactly satisfies the boundary conditions along the surface of the crack, but has convergence problems. Since the Williams' series is in terms of the radial distance from the crack tip raised to a positive power (except for the first symmetric and antisymmetric terms)

Table 2. The boundary conditions used in the boundary collocation solutions

Load case				
$X$	$-y$	$0$	$y < \frac{1}{2}, 0; y > \frac{1}{2}, \frac{1}{2} - y$	$-6y^2(y/3 - \frac{1}{2})$
$AB \frac{\partial X}{\partial x}$	$0$	$-6y^2(y/3 - \frac{1}{2})$	$0$	$0$
$X$	$y^2(y-2)$	$-6(a-3)y^2(y/3 - \frac{1}{2})$	$-y^2/2$	$-6y^2(y/3 - \frac{1}{2})$
$A'B' \frac{\partial X}{\partial x}$	$0$	$-6y^2(y/3 - \frac{1}{2})$	$0$	$0$
$X$	$-1$	$(a+x)$	$-\frac{1}{2}$	$1$
$BC \frac{\partial X}{\partial y}$	$-1$	$0$	$-1$	$0$
$X$	$-y - \frac{(y-1)^2}{2(q+1)} - \frac{3(q-1)(y-1)^2}{(q+1)^3} \times [(y-1)/3 + (q+1)/2]$	$(a+q) \{ 1 - \frac{6(y-1)^2}{(q+1)^3} \times [(y-1)/3 + (q+1)/2] \}$	$-(y - \frac{1}{2}) - \frac{(y-1)^2}{2(q+1)} - \frac{3q(y-1)^2}{(q+1)^3} \times [(y-1)/3 + (q+1)/2]$	$1 - \frac{6(y-1)^2}{(q+1)^3} \times [(y-1)/3 + (q+1)/2]$
$CD \frac{\partial X}{\partial x}$	$0$	$1 - \frac{6(y-1)^2}{(q+1)^3} \times [(y-1)/3 + (q+1)/2]$	$0$	$0$
$X$	$0$	$0$	$0$	$0$
$D - F \frac{\partial X}{\partial y}$ or $\frac{\partial X}{\partial y}$	$0$	$0$	$0$	$0$

convergence is poor or unattainable if the boundaries lie at a variety of distances from the crack tip. True mathematical convergence cannot be attained by the Gross and Srawley method and the solution eventually must diverge as the number of terms is increased. The most that can be hoped for is that the value of the stress intensity factor remains reasonably stationary or fluctuates about a constant value with a moderate increase in the number of terms retained.

For long flakes, the stress distribution in the flake some distance from the crack tip is very close to that given by the simple beam theory and it is possible to avoid introducing boundary conditions on the flake at a large distance from the crack tip. Consequently, whenever the flake length is greater than 3, the boundary conditions have been introduced along  $A'B'$  and  $E'F'$  rather than along  $AB$  and  $EF$  (see Fig. 2). Following Gross and Srawley [6] it is easier to use an integrated form of the boundary conditions and to specify Airy's stress function  $\chi$  and its gradient rather than the normal and shear stresses. The boundary conditions for the four load cases are given in Table 2.

Best convergence was obtained for more-or-less uniform spacing between collocation points around the boundary. Convergence was fine-tuned by making the distance between collocation points along the boundary  $EF$  somewhat greater than elsewhere on the boundaries. Even so we found it impossible to obtain convergence in the stress intensity factors for  $q > 10$  or  $a < 2$ . Since we know from elementary beam theory that the limiting values of the stress intensity factors for load cases 1 and 3 are only approached when  $q > 10$ , these limiting values could only be obtained by extrapolation of the collocation solutions.

2.3. The limiting values for the stress intensity factors at the tip of a growing flake

The limiting values of the stress intensity factor for load cases 2 and 4 are easy to obtain. For both cases there is a less than 1% change in the value of the stress intensity factors for

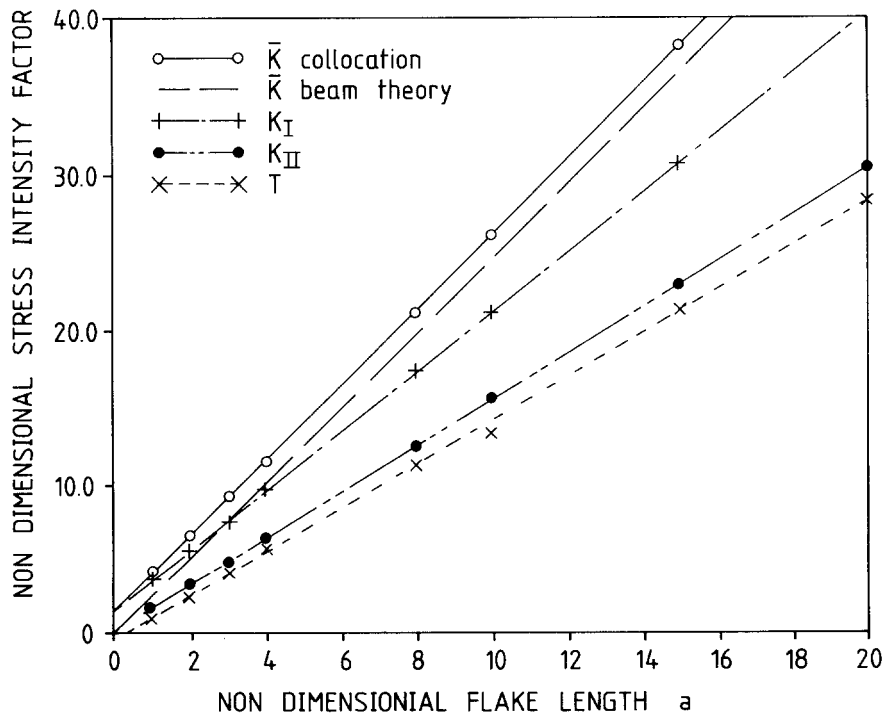


Figure 4. Stress intensity factors for load case 2.

Table 3. The limiting values of the stress intensity factor for large cores

Load case	1	2	3	4
$\bar{K}$	1.41	$1.50 + 2.44a$	0.707	2.44
$K_I$	-0.541	$1.68 + 1.92a$	0.419	1.92
$K_{II}$	1.33	$-0.17 - 1.50a$	0.570	-1.51
$T$	-1.38	$-0.66 + 2.27a$	-0.24	2.28



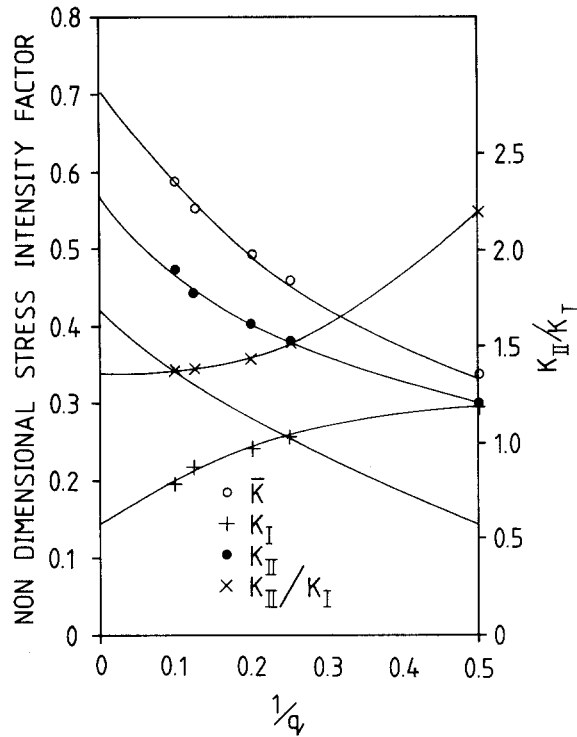


Figure 5. Stress intensity factors for load case 3.

$q > 3$ . The solution for case 4, where the flake is loaded by a bending moment, is also independent of the flake length when  $a > 2$ . Agreement for the modulus of the stress intensity factor obtained from simple beam theory and boundary collocation is remarkable for this latter case – the difference in the two solutions being less than 1%. For a flake loaded by a transverse load (case 2) the stress intensity factors are linear functions of the flake length (see Fig. 4 and Table 3). The slope of the modulus of the stress intensity factor line is almost precisely the same as that obtained from simple beam theory and, like the Gross and Srawley solution for a double cantilever beam specimen, has a small positive intercept on the zero axis.

The stress intensity factors for load case 1 and 3 are independent of the flake length for  $a > 2$ , but vary significantly with the size of the core. The modulus of the stress intensity factors is in good agreement with that obtained from simple beam theory (see Fig. 3) and we assume that the limiting value of the modulus of the stress intensity factors for these load cases is that given by simple beam theory. The stress intensity factors obtained from boundary collocation for  $a > 2$  are shown as functions of  $1/q$  in Figs. 5 and 6. The variation of  $K_I/K_{II}$  for small values of  $1/q$  is not large for load case 3 and the curve has been extrapolated to zero. The values of  $K_I$  and  $K_{II}$  for an infinite core have been calculated from the limiting value of the modulus  $\bar{K}$  obtained from simple beam theory and the extrapolated value of  $K_I/K_{II}$ . The variation of  $K_I/K_{II}$  with  $1/q$  for load case 1 is more pronounced and the limiting values have been calculated from load cases 3 and 4. Examination of Figs. 5 and 6 shows that the limiting values obtained by this means are in good agreement with the results from boundary collocation.

The limiting values of the stress intensity factors are summarized in Table 3. The second term in the Williams' series expansion  $T$ , which represents a constant stress parallel to the crack, has also been calculated (see Table 3).

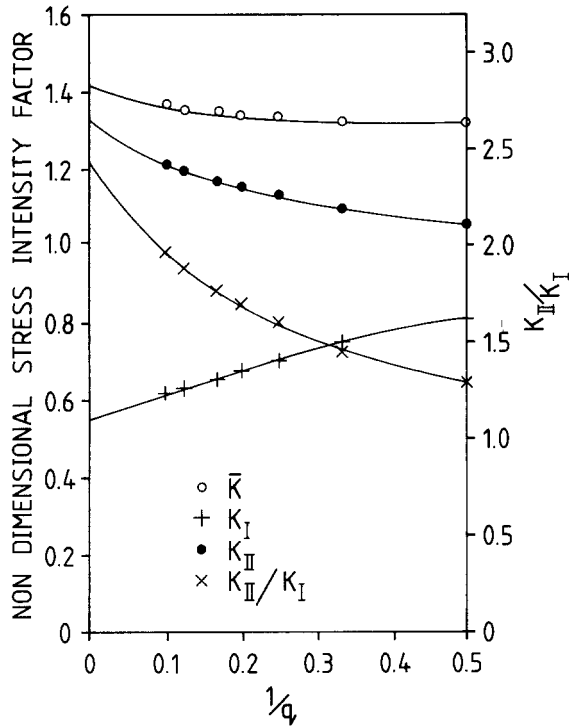


Figure 6. Stress intensity factors for load case 1.

### 3. Crack paths in flaking

There have been many descriptions of the path that cracks take in a brittle homogeneous and isotropic material. The earliest proposal, which is the one currently accepted, is that cracks propagate to extend perpendicular to the maximum circumferential stress [12–16]. Others have proposed a maximum energy release rate [18–20] or stationary strain energy density function [21–23]. One of us has pointed out in a previous paper [24] that all these criteria have the implication that a crack propagates so that it maintains a pure mode I stress field at its tip and are encompassed by the “criterion of local symmetry” [25–27]. Certainly any non-elastic deformation at the tip of the crack will affect the local stress distribution. It has been shown [13–16,20] that non-elastic deformation can be accommodated if the stress is examined not right at the crack tip but at a small characteristic distance from it. The more brittle the material the smaller is the material characteristic dimension  $r_c$ . Since the siliceous materials favoured for stone tools were extremely brittle, we neglect any effects of non-elastic deformation and will examine the stress field right at the crack tip. The velocity of crack propagation in flaking is relatively low [2,28] and hence dynamic effects can be neglected.

#### 3.1. Effect of force angle on the crack path

To maintain the crack path parallel to the free surface of the core it is necessary for the force angle to vary so that  $K_{II} = 0$ . Using the expressions for the stress intensity factor given in Table 3, the required force angle  $\phi$  has been calculated as a function of the flake length (see Fig. 7). As the flake develops it is necessary for the direction of the force to rotate to become nearly aligned with the free surface of the core. If the force angle is too

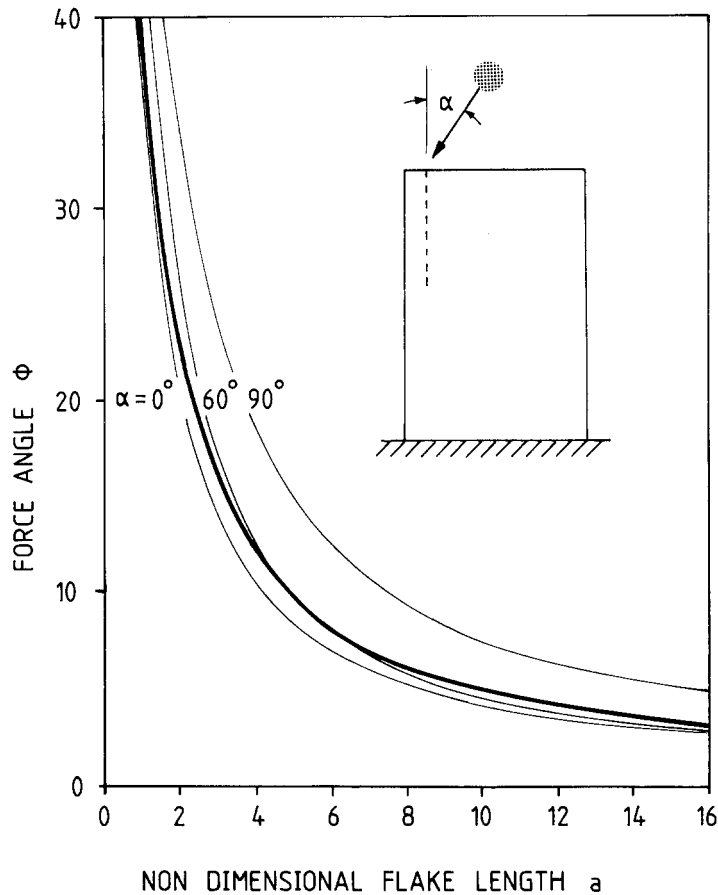


figure 7. Force angle as a function of flake length.

large the flake will hinge towards the free surface of the core. On the other hand, too small a force angle will cause intraflexion of the crack towards the interior of the core and produce what archaeologists term a plunging fracture. Although in a fracture mechanics sense the velocity of crack propagation is low, a stone-knapper could not possibly control the force angle during the fraction of a millisecond it takes to form a flake.

To check the accuracy of the prediction of the force angle required to produce a crack running parallel to the free surface of a core we performed some experiments on square glass plates cut down one side with a diamond saw to model a core with a partially formed flake. The apparatus to load this flake was designed to ensure that the force angle was maintained during the flake's final detachment (see Fig. 8). The glass plate was clamped between two supporting bars in a vice. Load arms (one of which is cut away in Fig. 8 for clarity) were pinned to a block that fitted on the top of the model flake and were loaded by a turnbuckle. A sharp natural crack was introduced at the bottom of the partial detachment by heating a small spot immediately below the saw cut with an electric soldering iron. By slowly tensioning the load arms it was possible to produce a semi-stable fracture. The crack paths resulting from various force angles for flakes of length approximately 5.5 times their thickness are shown in Fig. 9. The characteristic inflexion of the crack path that occurs as the crack nears the free surface of the core, though not important in the present paper, is also of interest. Such inflexions are common in bending fractures [20,29] and are often a feature on the terminations of flakes [30]. There are some anomalies in the crack paths shown in Fig. 9 caused most likely by an inability to produce

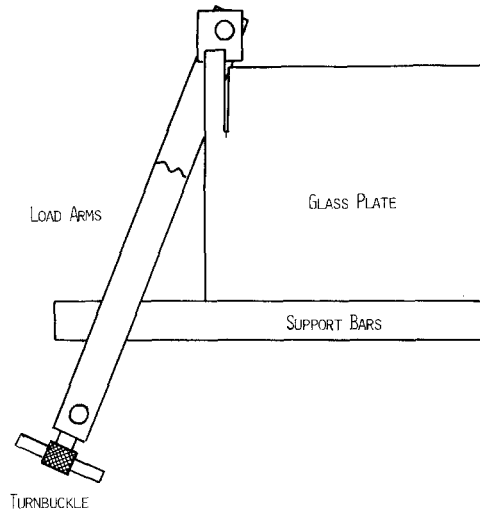


Figure 8. Constant force angle apparatus.

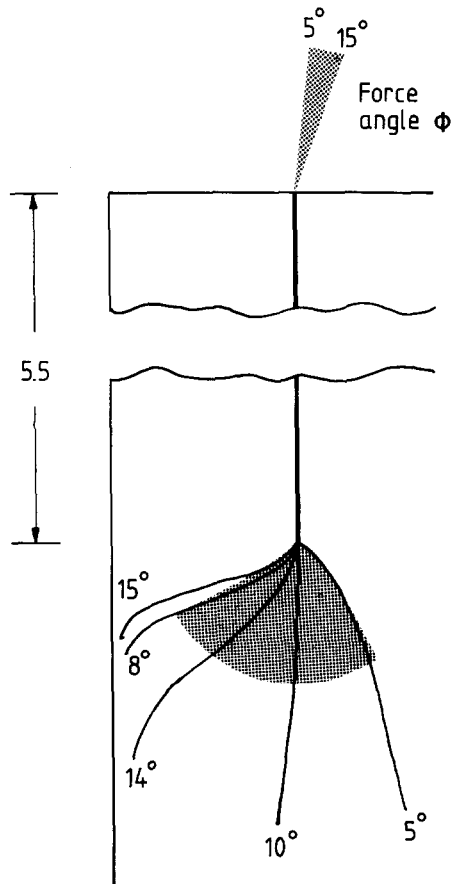


Figure 9. Crack paths as a function of force angle.

truly two-dimensional flakes. However, the trend is clear. Small force angles cause an intraflexion in the flake direction while larger angles cause the flake to hinge. The whole range in load angles is only  $10^\circ$ , but this small range causes a large difference in the crack paths.

For small crack growths the crack path can be estimated from a first order solution [24]. The crack will continue to run parallel to the surface of the core if  $K_{II} = 0$ , which gives a force angle of about  $9^\circ$ . The crack paths for other force angles are given by

$$y = \frac{\tan \theta}{\beta^2} \left\{ \exp(\beta^2 x) \operatorname{erfc}(-\beta x^{1/2}) - 1 - 2\beta \left( \frac{x}{\pi} \right)^{1/2} \right\} \quad (1)$$

where  $x$  and  $y$  are measured as shown in Fig. 8,  $\beta = (2\sqrt{2} T/K_I)$  and  $\theta$  is the root of the equation

$$\frac{\sin \theta}{3 \cos \theta - 1} + \frac{K_{II}}{K_I} = 0 \quad (2)$$

given by Erdogan and Sih [12]. The crack paths calculated from these equations for the extremes of the force angles ( $5^\circ$  and  $15^\circ$ ) are indicated by the shaded region in Fig. 9. These extreme values are in agreement with the experimental results which indicate that the force angle must vary during the formation of conchoidal flakes.

### 3.2. The effect of flake stiffness on the crack path

In percussion flaking with a hammer, the energy absorbed in the fracture process is small. Therefore, the direction of motion of the hammer can vary only slightly during the formation of the flake. The stone-knapper cannot change this direction in the extremely short time it takes to create the flake. The pressure flaking technique in reality involves an element of impulsive loading. The knapper in throwing part of his weight onto the flaking tool controls not the force angle, but the direction of the impulsive motion. Although the velocity of impact is very low, the kinetic energy is still considerable because a large part of the knapper's mass is involved. More delicate secondary flaking by pressure involves a similar impulsive motion, but with a smaller energy. Hence percussion and pressure flaking are mechanically very similar.

We have already shown that simple bending theory accurately models the formation of a flake. If the direction of motion of the hammer or flaking tool makes an angle of  $\alpha$  to the free surface of the core, then the force angle  $\phi$  as a function of the developing flake length  $a$  (assuming that the equations of bending apply for all flake lengths) is given by

$$\tan \phi = \frac{4 \tan \alpha + 3a}{a(3 \tan \alpha + 4a)}. \quad (3)$$

In Fig. 7 we superimpose the force angle defined by (3) on the force angle necessary to cause the crack to propagate parallel to the core's surface. The force angle is seen to be very insensitive to the direction with which the core is impacted because the flake is much more flexible in bending than in compression. For the range of striking angles commonly used in flaking ( $0^\circ$ – $60^\circ$ ), the force angle determined by the stiffness of the flake corresponds closely to those necessary to form long thin flakes. Hence thin flakes can be removed by impacting a core over a wide range of angles. It is this stiffness that determines the force angle appropriate for a flake's formation.

### 3.3. The stability of the crack path in flaking

The stiffness of the developing flake does not so precisely determine the force angle that the crack will have local symmetry at its tip when it is propagating exactly parallel to the

surface of the core. However, small discrepancies in angle can be accounted for by a self-correcting mechanism. If the crack should hinge toward the free surface, the negative bending moment caused by the direct component of force increases. This increase has the effect of making  $K_{II}$  positive which causes the crack to deflect back toward a parallel path. Crack intraflexion into the body of the core has a similar correcting mechanism. In part this self-correcting mechanism could be responsible for the undulations that are observed on the surfaces of conchoidal flakes (see Fig. 1).

The constant term  $T$  in the Williams' series expansion (which for a crack propagating parallel to the surface of the core is positive except for extremely short flakes) does have a potentially destabilizing effect [24]. However, what is important in determining the degree of path stability is the magnitude of the ratio  $T/K_I$ . This ratio is quite small for flakes growing parallel to the surface of a core. For example  $T/K_I = 0.426$  for a flake that has a length ten times its thickness, as compared with 1.33 for a DCB specimen of similar dimensions. Even in the unstable DCB specimen the crack deflection requires some distance to be apparent [30] and it is reasonable to believe that any instability in the crack path will be slight because the constant stress term  $T$  is positive. Indeed, others have argued that the condition  $T < 0$  for stability may be too severe for a real material. If there is non-elastic deformation at the crack tip the path can be stable even if  $T$  is slightly positive [16,20].

#### 3.4. *Experimental verification of the effect of the stiffness of the flake on the crack path*

To demonstrate that the force angle does decrease as the flake is formed, we have removed flakes from glass plates with an instrumented flaking tool (Fig. 10). This tool, which has a conical steel tip, was provided with strain gauges which enable the direct and transverse forces acting on it to be measured. The flaking experiments were performed in semi-dark-

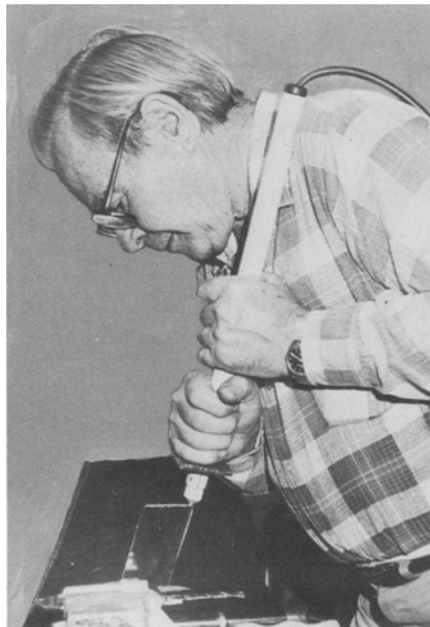


Figure 10. Flaking with an instrumented tool.

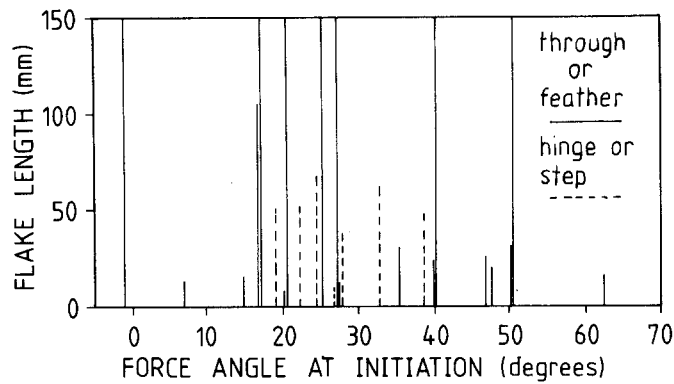


Figure 11. Flake length as a function of force angle at initiation.

ness under a photographic safety light and at the moment of flake initiation (sensed by the breaking of a line of conducting paint) a microflash was triggered and a photograph taken of the flaking tool to determine its orientation with respect to the glass plate. The forces acting on the indenter, together in some cases with indications of the positions of the crack tip from lines of conducting paint, were recorded on an oscilloscope.

Two sets of experiments were performed. The first was designed to record the forces at initiation and used the applied force to trigger the oscilloscope. In the second set of experiments the forces were measured during the propagation of the crack and the oscilloscope triggered from the break in a line of conducting paint. It was not possible to measure both initiation and propagation in the one experiment, because when the oscilloscope was triggered from the force on the tool, the time base had to be of comparatively long duration to avoid missing the initiation event and the propagation phase was compressed so much that it could not be interpreted. Conversely, initiation was missed when the oscilloscope was triggered from the break in a line of conducting paint. The force angles  $\phi$  have been calculated for both sets of experiments.

In Fig. 11 the length of the detached flake is shown as a function of the force angle at initiation. Flakes that have run the complete length of the glass plate (150 mm) were

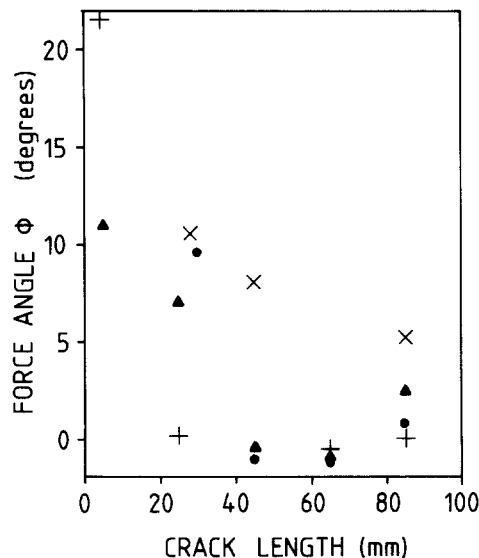


Figure 12. Measured force angle as a function of flake length.

produced for initial force angles varying from  $-1^\circ$  to  $51^\circ$ . In addition, so-called feather flakes (where the crack meets the surface of the core at a very small angle and never turns sharply towards the surface) were recorded for initiation force angles as large as  $65^\circ$ . Short hinge or step (arrested) flakes did sometimes occur if the initiation load angle was greater than  $19^\circ$ . However, even these flakes had a length at least ten times their thickness. Hence long flakes can be produced from impulses which initially apply the force over a wide range of angles.

The variation in force angle as the crack propagates is shown in Fig. 12. These results cannot be compared quantitatively with Fig. 7 because the thickness of the flakes is not constant over their length; nevertheless, the general qualitative trend for the force angle to decrease as the flake develops is unmistakable. The greater flexibility of the flake in bending causes the transverse force component to decrease rapidly with crack growth.

#### 4. Conclusions

Unless the direction of the flaking force is appropriate, the crack forming a flake will hinge outward toward the surface of the core or plunge inward. The required direction of the force required to keep the crack parallel to the surface of the core varies with the growth of the crack. Precise manual control of the flaking force is not possible. However, the stiffness of the partially formed flake dictates that the line of force shall be close to the angle required to cause the crack to propagate parallel to the surface of the core. The actual direction of the blow or impulse that detaches the flake has little effect on the crack path. Any discrepancies between the actual force angle and that required is translated into small undulations in the thickness of the resultant conchoidal flake. If the force angle is too large then the flake becomes thinner, causing a correcting increase in  $K_{II}$ . Conversely, too small a force angle causes the flake to thicken and decrease  $K_{II}$ .

Thus it can be seen that little skill is required to produce a usable conchoidal flake with a sharp cutting edge. The plan shape of such flakes can be very irregular. Naturally, the making of the beautiful, symmetrically flaked stone projectile points of late prehistoric times did require considerable knowledge and skill in flaking techniques. However, the angle at which the impulsive motion was applied could vary over a wide range even in the production of these delicate implements. Only the best stone was used to make such projectile points, so that secondary flake removals were unaffected by inhomogeneities and were predictable. A planned reduction sequence involving careful preparation of the platform from which small thin flakes were removed and the successive use of different flaking implements were much more important than the precise angle of the impulse.

It is self-evident that simple conchoidal flaking must be easy or it would not have appeared so early in our evolution. A hominid ancestor of modern Man, *Homo habilis*, made simple but perfectly usable flaked stone tools more than one and a half million years ago [32]. No doubt our remote ancestors used tools made from perishable materials such as wood and bone, but flaked stone tools were fundamental to their technology. It is tempting to speculate that Mankind may have had a different evolution if conchoidal flaking had not been made easy by the controlling effect of stiffness on the crack path.

#### Acknowledgements

This research was financed by the Australian Research Grants Scheme.

#### References

- [1] B. Lawn and R. Wilshaw, *Journal of Materials Science* 10 (1975) 1049–81.
- [2] A. Faulkner, *Mechanical Principles of Flintworking*, Doctoral dissertation, Washington State University (1972).



- [3] F. von Kerkhof and H. Müller-Beck, *Glastechnische Berichte* 42 (1969) 439–48.
- [4] J.G. Fonseca, J.D. Eshelby and C. Atkinson, *International Journal of Fracture Mechanics* 7 (1971) 435–47.
- [5] B. Cotterell and J. Kamminga, in *Lithic Use-Wear Analysis*, B. Hayden, Editor, Academic Press (1979) 97–112.
- [6] J. Kamminga, *Over the Edge. Functional Analysis of Australian Stone Tools*, Occasional Papers of Anthropology, Anthropology Museum, University of Queensland, 12 (1982).
- [7] L.H. Keeley, *Experimental Determination of Stone Tool Uses*, University of Chicago Press (1980).
- [8] B. Gross and J.E. Srawley, *Stress-Intensity Factors by Boundary Collocation for Single Edge-Notch Specimens Subject to Splitting Forces*, NASA TN-D3295 (1966).
- [9] M.J. Fernandes, Determination of the Stress Intensity Factors, and the First Three Non-Zero Matrix Coefficients for the Compact Tension Specimen Subjected to Mode I and Mode II Crack Tip Loading, Master of Engineering Science thesis, Sydney University (1977).
- [10] R.M.L. Foote and V.T. Buchwald, *International Journal of Fracture* 39 (1985).
- [11] M.L. Williams *Journal of Applied Mechanics* 24 (1957) 109–14.
- [12] F. Erdogan and G.C. Sih, *Journal of Basic Engineering* 85 (1963) 519–27.
- [13] I. Finnie and A. Saich, *International Journal of Fracture* 9 (1973) RCR 484–6.
- [14] P.D. Ewing and J.G. Williams, *International Journal of Fracture* 10 (1974) RCR 135.
- [15] P.D. Ewing, J.L. Swedlow and J.G. Williams, *International Journal of Fracture* 12 (1976) 85–93.
- [16] R. Streit and I. Finnie, *Experimental Mechanics* 20 (1980) 17–23.
- [17] B. Cotterell, *International Journal of Fracture Mechanics* 1 (1965) 96–103.
- [18] M.C. Hussain, S.L. Pu and J. Underwood, in *Fracture Analysis*, Proceedings of the 1973 National Symposium on Fracture Mechanics, Part II, ASTM STP 560 (1973) 2–28.
- [19] K. Palaniswamy and W.G. Knauss, in *Mechanics Today*, S. Nemat-Nasser, Editor, Vol. 4, Pergamon Press (1978) 87–148.
- [20] H.J. Schindler and M. Sayir, *International Journal of Fracture* 25 (1984) 95–107.
- [21] G.C. Sih, *Engineering Fracture Mechanics* 5 (1973) 365–77.
- [22] G.C. Sih, in *Mechanics of Fracture, Vol. 1, Methods, Analysis and Solutions of Crack Problems*, Noordhoff (1973).
- [23] G.C. Sih, *International Journal of Fracture* 10 (1974) 305–21.
- [24] B. Cotterell and J.R. Rice, *International Journal of Fracture* 16 (1980) 155–69.
- [25] N.V. Banichuk, *Izv. An SSR, MIT*, 7, 2 (1970) 130–7 (in Russian).
- [26] R.V. Gol'dstein and R.L. Salganik, *Izv. An SSR, MIT*, 7, 3 (1970) 69–82 (in Russian).
- [27] R.V. Gol'dstein and R.L. Salganik, *International Journal of Fracture* 10 (1974) 507–23.
- [28] D.E. Crabtree, *American Antiquity* 33 (1968) 466–78.
- [29] V.K. Kinra and H. Kolsky, *Engineering Fracture Mechanics* 9 (1977) 423–33.
- [30] B. Cotterell and J. Kamminga, *Finals on Stone Flakes*, *Journal of Archaeological Science*, in press.
- [31] B. Cotterell, *International Journal of Fracture* 2 (1966) 526–33.
- [32] G.L. Isaac, in *Advances in World Archaeology*, F. Wendorf and A.E. Close, Editors, 3 Academic Press, New York (1984) 1–87.

## Résumé

Les outils en pierre taillée sont les témoignages les plus durables et, dès lors, les plus courants à disposition des archéologues pour traquer le développement des premiers hommes. On n'a cependant pas encore décrit les mécanismes essentiels de la formation d'une écaille conchoïdale. Pour créer avec succès une écaille relativement mince qui ne soit pas prématurément trop courte, il faut que la direction de la force d'écaillage soit relativement précise. On démontre que la direction de cette force est essentiellement déterminée par la raideur de l'écaille, l'angle réel de percussion ayant, pour sa part, un effet relativement peu important. Il est possible de réaliser des écailles longues et minces dès lors que la direction de la force d'écaillage est très voisine de celle nécessaire à produire une symétrie locale à l'extrémité d'une fissure se propageant parallèlement à la surface de la pierre.